

AD-753 429

THE ROLE OF INTERNAL CONVERSION
ELECTRONS IN GADOLINIUM-EXPOSURE
NEUTRON IMAGING

A. A. Harms, et al

McMaster University
Hamilton, Ontario, Canada

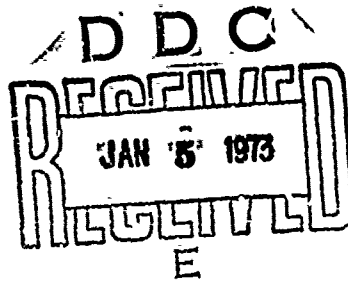
3 January 1972

DISTRIBUTED BY:

NTIS

National Technical Information Service
U. S. DEPARTMENT OF COMMERCE
5285 Port Royal Road, Springfield Va. 22151

AD 753429



The Role of Internal Conversion Electrons in Gadolinium-Exposure Neutron Imaging

A. A. Harms

Department of Engineering Physics, McMaster University, Hamilton, Ontario, Canada

and

G. R. Norman

Faculty of Medicine, McMaster University, Hamilton, Ontario, Canada

(Received 3 January 1972)

A radiation conversion and radiation transport model applicable to gadolinium-exposure neutron imaging is formulated. The resultant linear optical density representation is found to be in good agreement with experiment. The distinct conversion-electron contributions thus identified confirm the supposition about the dominant mode of image formation in gadolinium-exposure neutron imaging.

INTRODUCTION

The increasing availability of intense neutron sources has contributed to a broad interest in experimental neutron radiography.¹⁻⁵ Recently, studies have been reported which elucidate the mathematical-geometrical description of the optical image.⁶⁻⁸ These studies suggest that a need exists for a model of the dominant radiation conversion and transport processes which contribute to the optical film density. Herein we formulate and test a simplified radiation conversion and radiation transport model specifically relevant to gadolinium-exposure neutron radiography.

The experimental arrangement of the neutron radiographic system considered is schematically represented in Fig. 1. Neutrons are assumed to pass largely unattenuated through the film emulsion and aluminum foil and thereupon become strongly attenuated in the gadolinium conversion foil. The neutron-nucleus absorption process in the converter foil thereupon produces a source of conversion radiation which subsequently leads

to film blackening. The discussion on the type of radiation which eventually leads to the optical density in the film is deferred to the end of this paper.

RADIATION TRANSPORT MODEL

We consider the energy-dependent neutron-nucleus interaction density at the point P in the converter. If we designate this quantity by $F(x_1)$, then, in this one-dimensional representation, we may write

$$\begin{aligned} F(x_1) &= \int_0^\infty \Sigma(E) \phi(E, x_1) dE \\ &= \int_0^\infty \Sigma(E) \phi(E, x_1) \exp[-\Sigma(E)(x_1 - x_0)] dE \\ &= \Sigma \phi(x_1) \exp[-\Sigma(x_1 - x_0)]. \end{aligned} \quad (1)$$

In this expression we use Σ as the appropriately energy-averaged macroscopic absorption cross section for neutrons in gadolinium foil and $\phi(x_1)$ represents the scalar neutron flux on the x_1 plane.

To obtain an expression for the production density of

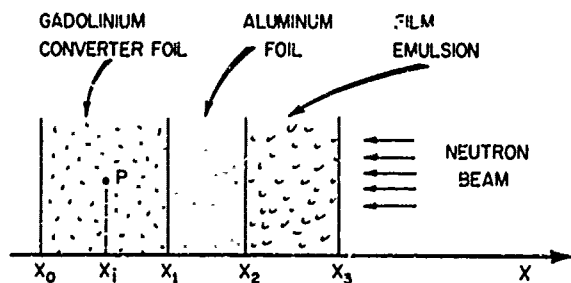


FIG. 1. Geometric and material arrangement used for neutron radiographic imaging.

conversion radiation, designated by $R(x_1)$, we assume that this quantity is directly proportional to the neutron-nucleus interaction density:

$$R_j(x_1) = Y_j F(x_1) = Y_j \Sigma \phi(x_1) \exp[-\Sigma(x_1 - x_1)]. \quad (2)$$

In this equation we introduce the subscript "j" to emphasize that distinct conversion radiation energy groups may be produced. Thus, Y_j is equal to the yield fraction of the jth radiation energy group produced in this conversion process.

The radiation flux at x_2 which contributes to the optical density in the film emulsion, defined by $J_j(x_2)$, will depend upon the transport kernel for the specific radiation energy group in question. If we symbolically define this positive dimensionless function by $K_j(x_1 \rightarrow x_2)$, we may combine this kernel with the radiation production density rate by an integration over the gadolinium thickness to yield an expression for the radiation flux at x_2 :

$$\begin{aligned} J_j(x_2) &= \int_{x_1}^{x_2} Y_j \Sigma \phi(x_1) \exp[-\Sigma(x_1 - x_1)] K_j(x_1 \rightarrow x_2) dx_1 \\ &= Y_j \Sigma \phi(x_1) \int_{x_1}^{x_2} \exp[-\Sigma(x_1 - x_1)] K_j(x_1 \rightarrow x_2) dx_1. \end{aligned} \quad (3)$$

In this expression it is necessary to emphasize the limited range of permissible integration of the transport kernel for the jth radiation energy group; for this reason we specify the lower limit of integration by x_1 .

In the present analysis we assume that the kernel for our radiation transport model can be adequately approximated by a positive definite linear relationship of the form

$$K_j(x_1 \rightarrow x_2) = |1 - (\rho_{Gd}/R_{Gd,j})(x_1 - x_1)| |1 - (\rho_{Al}/R_{Al,j})(x_2 - x_1)|, \quad (4)$$

where $R_{Gd,j}$ and $R_{Al,j}$ are the ranges in gadolinium and aluminum, respectively, in units of mass per area; the densities of gadolinium and aluminum are represented by ρ_{Gd} and ρ_{Al} .

If the radiation groups can be considered to be contained in a relatively narrow energy range, then we may use the common model that the range, when expressed in units of mass per area, is independent of the material. Hence we write

$$R_{Gd,j} = R_{Al,j} = R_j. \quad (5)$$

Upon substitution of Eq. (5) into Eq. (4) and subsequently into Eq. (3) we obtain an explicit expression for the radiation flux at x_2 :

$$\begin{aligned} J_j(x_2) &= Y_j \Sigma \phi(x_1) \int_{x_1}^{x_2} \exp[-\Sigma(x_1 - x_1)] \\ &\quad \times \left(\frac{R_j - \rho_{Gd}(x_1 - x_1)}{R_j} \right) \left(\frac{R_j - \rho_{Al}(x_2 - x_1)}{R_j} \right) dx_1 \\ &= [Y_j \phi(x_1) \exp(-\Sigma x_1) / R_j^2] [R_j - \rho_{Al}(x_2 - x_1)] \\ &\quad \times \{ (R_j - \rho_{Gd} x_1) [\exp(\Sigma x_1) - \exp(\Sigma x_2)] \\ &\quad + \rho_{Gd} \exp(\Sigma x_1) (x_1 - 1/\Sigma) - \rho_{Gd} \exp(\Sigma x_2) (x_2 - 1/\Sigma) \}. \end{aligned} \quad (6)$$

This expression for the radiation flux at x_2 may be symbolically written as

$$J_j(x_2) = Y_j [\phi(x_1) / R_j^2] G(\Sigma, x_1, x_2, \rho_{Gd}) [R_j - \rho_{Al}(x_2 - x_1)], \quad (7)$$

where $G(\Sigma, x_1, x_2, \rho_{Gd})$ is a function of the gadolinium converter only. Since the radiation flux at x_2 will subsequently impinge on the film emulsion then—assuming that film blackening occurs in the linear exposure range—the resultant optical density will be proportional to the radiation flux. Therefore, the experimentally measured optical density resulting from the jth radiation energy group, designated by D_j , can be represented by

$$D_j = \epsilon_j Y_j [\phi(x_1) / R_j^2] G(\Sigma, x_1, x_2, \rho_{Gd}) [R_j - \rho_{Al}(x_2 - x_1)], \quad (8)$$

where ϵ_j is the emulsion response parameter.

From Eq. (8) it is evident that, for a given neutron radiographic imaging system, the optical density D_j for the jth radiation energy group will decrease linearly with increasing aluminum thickness. If there are several such energy groups, then the resultant optical density constitutes the summation effect of such linear contributions. Thus, the individual radiation energy groups

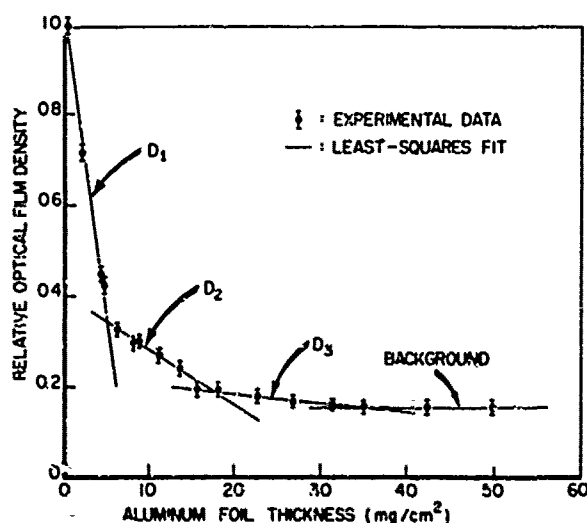


FIG. 2. Relative optical film density as a function of aluminum thickness.

TABLE I. Range and optical density contribution of conversion radiation.

Radiation energy group (<i>j</i>)	Conversion radiation range, R_j (mg/cm ²)	Relative contribution to optical density, D_j (arbitrary scale)	Optical density contribution (normalized to 100%)
1	5.5 ± 0.3	0.599 ± 0.025	71.8%
2	16 ± 2	0.162 ± 0.020	19.4%
3	32 ± 8	0.073 ± 0.016	8.8%

should be experimentally discernable if they are sufficiently distinct.

EXPERIMENTAL RADIATION IMAGING

To test the validity of the analysis leading to Eq. (8), we conducted a series of neutron radiographic experiments using the imaging system schematically represented in Fig. 1. The converter consisted of a 25- μ -thick high-purity gadolinium foil. Aluminum foils were assembled to vary in thickness from 2 to 50 mg/cm². A neutron flux of $\sim 5 \times 10^6$ /cm²/sec was extracted from the McMaster University Nuclear Reactor through a 2.5-cm-diam vertical access tube.

Optical film density is not an ideal indicator of radiation energy group exposure. To circumvent some of the potential problems, we undertook several precautionary steps. The effects of developer conditions were minimized by batch development. From preceding exposure calibration measurements, it was possible to select irradiation times which ensured that the resulting film blackening would fall within a narrowly defined range. The ratios of times required to obtain the same film blackening as that required for a standard was taken as a relative measure of optical film density. The usefulness of this latter step rests on the assumption that "reciprocity failure" does not exist for the image formation process; this has been found to be generally appropriate for neutron radiography.⁸

The experimental results from the neutron radiographic measurements are shown in Fig. 2. It is graphically evident that the relative optical density is resolvable into three distinct linear components. By the methods of least squares, we have calculated the effective ranges, R_j , of these three radiation energy groups together with their relative intensities at x_1 . These results are summarized in Table I.

Equation (8) can be reduced to yield information on the product of the emulsion performance parameter and the conversion radiation yield given by $\epsilon_j Y_j$. For this calculation we specify zero aluminum thickness and impose a lower limit of integration by setting

$$x_j = x_1 - R_j / \rho_{\text{Al}}. \quad (9)$$

Equation (8) now reduces to

$$D_j = \epsilon_j Y_j \phi(x_1) \{1 - [(1 - e^{-\alpha_j}) / \alpha_j]\}, \quad (10)$$

where

$$\alpha_j = R_j \Sigma / \rho_{\text{Al}}, \quad (11)$$

with R_j satisfying

$$R_j \leq (x_1 - x_0) \rho_{\text{Al}}. \quad (12)$$

Rearranging Eq. (10) yields an explicit expression for the parameter $\epsilon_j Y_j$:

$$\epsilon_j Y_j = D_j \{1 - [(1 - e^{-\alpha_j}) / \alpha_j]\}^{-1}. \quad (13)$$

Herein we have normalized the optical film density to $D_j = D_j / \phi(x_1)$.

The calculations leading to the results enumerated in Table I have provided both D_j and R_j ; the values used for Σ and ρ_{Al} were 1400 cm⁻¹ and 7.89 g/cm³. Using these parameters, we have calculated the parameter $\epsilon_j Y_j$, see Table II.

DISCUSSION AND CONCLUSION

The system and procedures used in this investigation are typical of those used in direct-exposure neutron radiography when gadolinium is used as the converter medium. The experimental results, therefore, provide evidence concerning the radiation transport and radiation recording process which characterize such radiographic techniques.

It is, however, informative to compare our experimental result obtained from this work with a result from a recent beta-spectroscopy study which employed gadolinium exposed to a neutron beam.¹⁰ From this investigation by Feigl and Rauch it is also clear that three conversion-electron groups dominate the radiation spectrum. We have extracted the intensities of the lowest two energy groups for the several gadolinium-foil thicknesses and find that their ratio varies from 6.0 to 8.0 with an average of 6.8.¹¹ The most appropriate data from our work corresponding to this ratio are given by the performance-yield parameters, Table II:

$$\epsilon_1 Y_1 / \epsilon_2 Y_2 = 7.1. \quad (14)$$

The agreement between these independent results suggests that the emulsion performance parameter, ϵ_j , may not be strongly energy dependent for the range of energies involved and that the conversion electrons represent the dominant form of radiation which contributes to film blackening in gadolinium-exposure neutron radiography.

Based on the conclusion that the conversion electrons represent the dominant radiation in this neutron radiographic process, one can use the experimentally measured radiation ranges, Table I, to calculate the energies of the electron groups. We have evaluated these energies using the Katz-Penfold¹² empirical correlation and find that the energies, in order of decreasing opti-

TABLE II. Performance-yield parameter for each conversion radiation energy group.

Radiation energy group (<i>j</i>)	Performance-yield parameter, $\epsilon_j Y_j$ (normalized to 100%)
1	83.2%
2	11.8%
3	5.0%

cal density contribution, are given by 64, 135, and 190 keV.

Finally, we point out that the design of improved imaging devices for gadolinium-exposure neutron radiography should be guided by the experimental results found in this investigation. The parameters which appear to be of greatest importance are the various contributions to optical density of the several radiation energy groups, i. e., 71.8%, 19.4%, and 8.8%, together with their corresponding ranges given by 5, 5, 18, and 32 mg/cm².

ACKNOWLEDGMENTS

The authors would like to thank T. J. Kennett for useful discussions on the subject. Part of this work was supported by the Defence Research Board of Canada.

¹H. Berger, *Neutron Radiography* (Elsevier, New York, 1965).

²J. P. Barton, *Trans. Am. Nucl. Soc.* 10, 443 (1967).

³M. R. Hawkesworth and J. Walker, *J. Mater. Sci.* 4, 817 (1969).

⁴M. Brown and P. B. Parks, *Am. J. Roentgenol.* 106, 482 (1969).

⁵W. L. Whittmore, J. E. Larsen, and J. R. Shoptaugh, *Materials Evaluation* 24, 93 (1971).

⁶W. L. Parker, P. A. Summers, and J. A. Ray, *Trans. Am. Nucl. Soc.* 14, 530 (1971).

⁷M. J. Flynn (private communication).

⁸B. K. Garside and A. A. Harms, *J. Appl. Phys.* 42, 5161 (1971).

⁹M. K. Hawkesworth, *J. Sci. Instr.* 2(2), 673 (1967).

¹⁰B. Feigl and H. Rauch, *Nucl. Instr. Methods* 61, 349 (1968).

¹¹High resolution studies by L. V. Groshev, A. M. Demidov, V. A. Ivanov, V. N. Lutsenko, and V. I. Pelekhov [*Izv. Akad. Nauk, SSSR, Ser. Fiz.* 26, 1118 (1962)] also indicate three dominant peaks near the energies found in this study. These results suggest that the intensity ratio could be larger.

¹²L. Katz and A. S. Penfold, *Rev. Mod. Phys.* 24, 28 (1952).

ACCESSION for	
ATIS	W. H. C. H. R. <input checked="" type="checkbox"/>
DOC	EFF. SER. <input checked="" type="checkbox"/>
UNCLASSIFIED	<input type="checkbox"/>
IDENTIFICATION	
BY	
DISTRIBUTION AVAILABILITY CODED	
Dist.	ASPL 2
A/21	